Available online at www.sciencedirect.com
SCIENCE DIRECT
Coordination Chemistry Reviews 250 (2006) 1804–1818
COORDINATION CHEMISTRY REVIEWS
www.elsevier.com/locate/ccr

Review

Coordination effects of nitroxide radicals in transition metal and lanthanide complexes

Sumio Kaizaki *

Department of Chemistry, Graduate School of Science, Osaka University, 1-1 Machikaneyamachyo, Toyonaka, Osaka 560-0043, Japan

Received 16 September 2005; accepted 23 February 2006
Available online 18 April 2006

Contents

Abstract

The coordination effects of the magnetic interaction between a paramagnetic transition metal or lanthanide ion and radical ligand(s) upon the spectroscopic (chiroptical and/or luminescence) properties will be described and discussed mainly for the heteroleptic complexes $[M(L)(X)_2]$ (M = Ni(II), Co(II), Cr(III), Ln(III); L = nitroxide radicals such as NIT2py(2-(2-pyridyl)-4,4,5,5-tetramethyl-4,5-dihydro-1H-imidazolyl-3-oxide-1-oxyl) or IM2py (2-(2-(pyridyl)-4,4,5,5-tetramethyl-4,5-dihydro-1H-imidazol-1-oxy), X = β-diketonates). For the Ni(II), Cr(III) or Co(II) complexes, we show how the orbital orthogonality or overlap between the $d_\sigma(e_g)$ or $d_\pi(t_{2g})$ of the metal ion and the SOMO (singly occupied antibonding π molecular orbital) of the nitroxides is relevant to the magnetic interactions associated with the spin-forbidden d–d transition intensity enhancement and/or the newly appeared d-SOMO metal-to-ligand charge transfer (MLCT) band. This is discussed in terms of the exchange mechanism or Valence Bond Configurational Interaction (VBCI) model. From the magnetic interactions for the Cr(III) with monodentate NIT*n*py and IM*n*py ($n = 3$ or 4) and their spectroscopic properties, the appearance of MLCT state is found to be a necessary and sufficient condition for the spin-forbidden transition intensity enhancement according to the spin-polarization mechanism. The lowest excited state magnetic interaction of the Cr(III) complexes was found to be larger than that of the ground state and discussed also on the basis of VBCI model. The magnetic circular dichroism (MCD) intensity enhancement of the intraligand singlet–triplet transitions in the ancillary acetylacetonate was examined in conjunction with the ligand-to-ligand charge transfer (LLCT) for the Ni(II) complexes. The intraligand transition of the nitroxide radicals was examined in connection with the luminescence behavior of the lanthanide(III) complexes.

Keywords: Magnetic interactions; Spin-forbidden ligand field transitions; MLCT; The lowest excited state magnetic interaction; Singlet–triplet transition in ancillary ligands; LLCT; Luminescence; MCD

* Tel.: +81 668505408; fax: +81 668505408.
E-mail address: kaizaki@chem.sci.osaka-u.ac.jp.

0010-8545/$ – see front matter © 2006 Elsevier B.V. All rights reserved.
doi:10.1016/j.ccr.2006.02.029

1. Introduction

The magnetic and spectroscopic properties in spin-coupled systems such as multinuclear paramagnetic metal complexes or paramagnetic metal complexes with paramagnetic radical ligands have been investigated from the stand point of coordination chemistry focusing on biological and material sciences [1–12]. In biological systems, metalloproteins with polynuclear active sites and some copper metal enzymes with phenoxyl radicals such as galactose oxidase show peculiar magnetic and spectroscopic properties [9], or are relevant because of one electron oxidation centered on either the metal or ligand [10]. From the viewpoint of molecular materials leading to molecular magnets [1–8] and molecular switches including the spin-crossover phenomena [13], the transition metal clusters or complexes with nitroxide monoradicals or nitroxide–semiquinone biradicals are expected to be appropriate promising targets. The most distinctive aspects of optical spectra in the spin-exchange systems are the intensity enhancement of the spin-forbidden ligand field d–d transition in exchange coupled polynuclear or one-dimensional, two-dimensional complexes [2] and the dihydroxo bridge Cr–Cr dimers [1,15]. For example, $Mn^{II}Cu^{II}_3$ tetranuclear complexes [12] and $[L_3Cr(OH)_3CrL_3]$ dimers [14] exhibit fairly strong formally spin-forbidden absorption bands. The (phenoxyl)chromium(III) complexes [10] gave too intense spin-forbidden bands to evaluate the exchange coupling constants with change of the coligand. However, there is no relevant study on nitroxide radical complexes, other than extensive magnetic studies aiming at construction of molecular magnets in terms of the so-called radical approach [6,7,16–21]. Recently, much attention has been paid to chiroptical spectra (circular dichroism (CD) and/or magnetic circular dichroism (MCD)) of the spin-coupled systems in connection with the magneto-chiral effect or chiral magnets [22]. Several CD spectra of chiral nitroxide radicals and their metal complexes have been reported [23]. It is very valuable to reveal the effect of coordination on the magneto-optical properties in order to understand the electronic spectra or the excited states of the nitroxide radical metal complexes.

Besides the magnetic interaction between the ground states in the spin-coupled systems, there are intramolecular magnetic interactions between the excited state in one moiety of the multi-spin systems and the ground state of the other one. This differentiates the excited state from the simple superposition of each moiety; e.g., the new appearance of so-called "dimer bands" due to the charge transfer (CT) transitions in Cu(II) and Fe(II) dinuclear complexes [9] and "intensity enhancement of the spin-forbidden d–d transitions" in the Mn(II)Cu(II) tetramers [12] or Cr(III) acetate trimer [24]. The former appearance of the CT is a necessary and sufficient condition to give the latter intensification in terms of a pair ion transition rather than a single ion transition [25]. The spin coupling in the excited states for the pair ion transition provides the same spin multiplicity as the ground states, leading to a formally spin-forbidden transition with the spin selection rule $\Delta S = 0$ in the single group theory [12,14,15,24], but not in the double group theory through the spin-orbit coupling for the single ion transition. In a reverse sense to the nitroxide complexes, the spin-forbidden singlet–triplet π–π^* transitions of diamagnetic organic ligands is enhanced by the influence of the coordinated paramagnetic metal ion; e.g., Cr(III) [26,27]. It is useful to know whether this same framework is applicable to Ni(II) complexes in consideration of the difference in magnetic d orbitals.

Moreover, configurational interaction (CI) between the spin-coupled ground levels and the CT levels results in antiferromagnetic or ferromagnetic properties; in other words, the interaction reveals the direct mechanism, as exemplified for the metal–metal CT in polynuclear complexes by Anderson [28], and later as claimed by Weihe and Güdel [29]. This description is equivalent to the consideration in terms of the Valence Bond Configurational Interaction (VBCI) model through the LMCT and/or metal–metal transitions developed by Solomon et al. [9,30].

There has been no systematic study of the simultaneous observation of the spin-forbidden transition intensity enhancement and CT, with the exception of only a few cases to which the proposed theoretical formulation were applied [16]. From these aspects, we have systematically investigated the magnetic and spectroscopic properties [31–40] of a series of transition metal and lanthanide complexes with nitroxide radical ligands; these have been reviewed [41]. More recently, this research has been extended to a magneto-optical study involving the luminescence and chiroptical spectra [42–44].

In this review, the latest topics including some chiroptical spectra will mainly be highlighted and discussed on the basis of the previous results [41].

Abbreviations for ligands:

Nitroxide radicals (Scheme 1):

NIT2py: 2-(2-pyridyl)-4,4,5,5-tetramethyl-4,5-dihydro-1H-imidazolyl-3-oxide-1-oxyl,

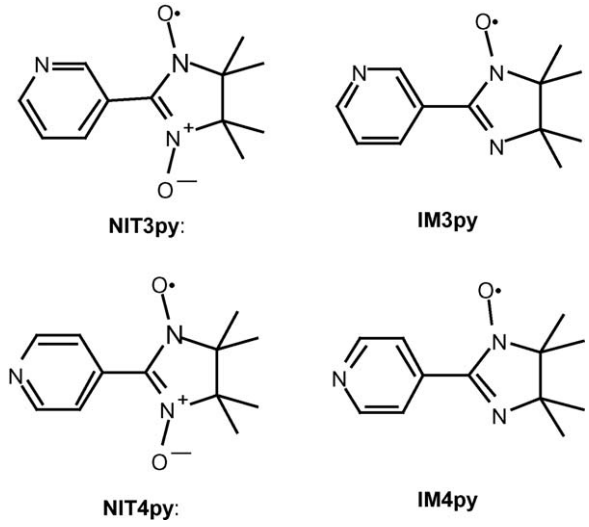

Scheme 1.

IM2py: 2-(2-(pyridyl)-4,4,5,5-tetramethyl-4,5-dihydro-1H-imidazol-1-oxy,
NIT3py or NIT4py: 4,4,5,5-tetramethyl-2-(3- or 4-pyridyl) imidazolin-1-oxyl 3-oxide,
IM3py or IM4py: 4,4,5,5-tetramethyl-2-(3- or 4-pyridyl)imidazolin-1-oxyl.

β-Diketones:

Hacac: 2,4-pentanedione,
Hdbm: 1,3-diphenyl-1,3-propanedione,
Hbzac: 1-phenyl-1,3-butanedione,
HacaMe: 3-methyl-2,4-pentanedione,
HacaEt: 3-ethyl-2,4-pentanedione,
Haca^{n}Bu: 3-*n*-buthyl-2,4-pentanedione,
HacaPh: 3-phenyl-2,4-pentanedione,
Hdpm: 2,2,6,6-tetramethyl-3,5-heptanedione,
HMehp: 6-methyl-2,4-heptanedione,
HacaPh: 3-phenyl-2,4-pentanedione,
Hhfac: 1,1,1,5,5,5-hexafluoro-2,4-pentanedione,
Htfac: 1,1,1-trifluoro-2,4-pentanedione,
Hbztfc: 4,4,4-trifluoro-1-phenyl-1,3-butanediketone,
Hthtfc: 4,4,4-trifluoro-1-(2-thienyl)-1,3-butanediketone,
Hnatfc: 4,4,4-trifluoro-1-naphthyl-1,3-butanediketone.

2. Magnetic interactions

2.1. Cr(III) and Ni(II) imino and nitronyl nitroxide radical complexes

2.1.1. Variation with β-diketonate ligands

The magnetic properties of various kinds of transition metal complexes were examined by temperature dependent magnetic susceptibility measurements. As was shown for the bis(hfac) mono-NIT2py [17] and IM2py [18] complexes, the magnetic interactions in [Ni(acac)$_2$(NIT2py)] or [Ni(acac)$_2$(IM2pyκ^2-*N*,*N*)] are antiferromagnetic and ferromagnetic, respectively (Table 1).

The important role of the orthogonality or overlap of the magnetic orbitals is confirmed by examining the magnetic properties of two linkage isomers for [Ni(acac)(tmen)(IM2py)]PF$_6$ (tmen = *N*,*N*′-tetramethylethylenediamine). A ferromagnetic interaction is observed for the five-membered IM2pyκ^2-*N*,*N* planar chelate and an antiferromagnetic interaction for the six-membered IM2pyκ^2-*N*,*O* non-planar chelate irrespective of the fact that the same ligands are involved [40] (Table 1). These facts agree with prediction on the basis of the orthogonality or orbital overlap between d(e_g) and radical SOMO π^* magnetic orbitals, for the former or latter species, respectively [32a,38,41].

Table 1
Magnetic and optical data of the NIT2py or IM2py Ni(II) and Cr(III) complexes

Compounds	J_{obsd} (g)[a]	ε_{SF}[b]	ε_{CT}[b]	$(\varepsilon_{SF}/\varepsilon_{CT})(\Delta E_{CT})^2/E_{CT}$[c]	J'_{EX}[d]
[Cr(acac)$_2$(NIT2py)]PF$_6$	−61.6 (2.00)	327	641	0.472	1500
[Cr(dbm)$_2$(NIT2py)]PF$_6$	−70.0 (2.00)	325	648	0.475	1950
[Cr(bzac)$_2$(NIT2py)]PF$_6$	−30.2 (2.01)	285	589	0.447	1800
[Cr(acaMe)$_2$(NIT2py)]PF$_6$	−9.05 (2.06)	230	504	0.429	1800
[Cr(acaPh)$_2$(NIT2py)]PF$_6$	−19.4 (2.02)	234	479	0.460	1770
[Cr(dpm)$_2$(NIT2py)]PF$_6$	−98.6 (2.00)	346	631	0.500	1530
[Cr(acaEt)$_2$(NIT2py)]PF$_6$	−36.5 (2.02)	265	536	0.477	
[Cr(aca^{n}Bu)$_2$(NIT2py)]PF$_6$	−12.3 (2.01)	279	567	0.462	
[Cr(Mehp)$_2$(NIT2py)]PF$_6$	−49.0 (2.00)	337	660	0.478	4340
[Cr(acac)$_2$(IM2py)]PF$_6$	−188 (2.01)	146	923	0.203	3600
[Cr(acaMe)$_2$(IM2py)]PF$_6$	−102 (2.03)	191	1367	0.241	4100
[Cr(acaPh)$_2$(IM2py)]PF$_6$	−119 (2.01)	184	1160	0.255	
[Cr(dbm)$_2$(IM2py)]PF$_6$	−96.4 (2.05)	160	1044	0.210	
[Ni(acac)$_2$(NIT2py)]	−219.4 (2.34)	448	887	0.325	
[Ni(bzac)$_2$(NIT2py)]	−223.8 (2.38)	465	870	0.319	
[Ni(dbm)$_2$(NIT2py)]	−206.5 (2.06)	472	894	0.315	
[Ni(tfac)$_2$(NIT2py)]	−207.6 (2.24)	258	583	0.261	
[Ni(hfac)$_2$(NIT2py)]	−167.0 (2.27)	111	417	0.148	
[Ni(acac)$_2$(IM2py)]	41.2 (2.12)	11.6	107	0.119	
[Ni(dbm)$_2$(IM2py)]	0.397 (2.13)	8.91	79.9	0.123	
[Ni(tfac)$_2$(IM2py)]	95.3 (2.15)	4.86	44.9	0.133	
[Ni(hfac)$_2$(IM2py)]	71.2 (2.13)	4.92	43.9	0.129	
[Ni(acac)(tmen)(IM2py-κ^2*N*,*O*)]PF$_6$	−135 (2.14)				
[Ni(acac)(tmen)(IM2py-κ^2*N*,*N*)]PF$_6$	98.3 (2.18)				

[a] Observed *J* values (cm^{-1}).
[b] Molar absorption coefficient for the spin-forbidden and MLCT transition, respectively (mol^{-1} dm^3 cm^{-1}).
[c] $(\varepsilon_{SF}/\varepsilon_{CT})(\Delta E_{CT})^2/E_{CT} \propto J_{AF}/10^3$ cm^{-1} where E_{CT} is the MLCT transition energy/10^3 cm^{-1} and ΔE_{CT} is the energy difference between the spin-forbidden and MLCT transition/10^3 cm^{-1}.
[d] $J'_{EX} = E_{SF} - E_{lum}$ (cm^{-1}) for the energy gap in the lowest excited state estimated from the difference between the spin-forbidden band E_{SF} and the luminescence peaks E_{lum}.

The difference in magnitude of the antiferromagnetic interaction for both $[Cr(acac)_2(NIT2py)]^+$ and $[Cr(acac)_2(IM2py\kappa^2\text{-}N,N)]^+$ can also be interpreted in the same manner. A decrease in overlap with the t_{2g} orbital for the non-planar chelate of the former NIT2py suppresses the antiferromagnetic interaction compared with the planar chelate of the IM2py [38,41].

For the chelated NIT2py or IM2py radical metal complexes with various kinds of β-diketonates, the variation of the β-diketonato coligands could afford valuable information on the spectroscopic behavior as well as on the magnetic interactions between a paramagnetic metal ion and NIT2py or IM2py [32a,35,38,41].

The magnetic coupling constants J_{obs} between a paramagnetic metal ion and nitroxide radical range from −207 to $-224\,cm^{-1}$ for the bis(β-diketonato)(NIT2py)Ni(II) complexes; from +0.400 to $+95.3\,cm^{-1}$ for the bis(β-diketonato)(IM2py)Ni(II) complexes; from −9.05 to $-98.6\,cm^{-1}$ and from −96.4 to $-188\,cm^{-1}$ for the NIT2py and IM2py Cr(III) complexes, respectively (Table 1).

The differences in magnitude of the magnetic interactions are found to be $|J_{obs}(NIT)| > |J_{obs}(IM)|$ for the Ni(II) complexes and $|J_{obs}(NIT)| < |J_{obs}(IM)|$ for the Cr(III) complexes. This can be accounted for by postulating both the antiferromagnetic and ferromagnetic contributions $J_{obs} = J_{ANT} + J_F$ through the orbital orthogonality or overlap between the magnetic d orbital and the SOMO π^*, LUMO π^* or HOMO π in the nitroxide radicals in terms of the exchange mechanism. The reverse behavior in the inequality relations for $|J_{obs}|$ between the Ni(II) and Cr(III) complexes results from the difference in magnetic orbitals, $t_{2g}(d_\pi)$ for Cr(III) and $e_g(d_\sigma)$ for Ni(II), which are orthogonal to each other.

The large diversity of J values with change of β-diketonate ligands is correlated with the spin-forbidden transition intensities as compared with the monodentate pyridyl coordinating NIT3py or NIT4py or IM3py or IM4py Cr(III) complexes in Section 2.1.4.

2.1.2. The charge transfer band and the spin-forbidden d–d transitions

The visible absorption spectra of [Ni(β-diketonato)$_2$(NIT2py)], [Ni(β-diketonato)(tmen)(NIT2py)]$^+$ and [Cr(β-diketonato)$_2$(NIT2py)]$^+$ at $16.0–19.0 \times 10^3\,cm^{-1}$ have characteristics with spacing of about $2000\,cm^{-1}$ as a peak or a shoulder, which are different from the n–π^* intraligand transitions of the ligand itself and the ligand field transitions of the non-radical complexes as shown in Figs. 1 and 2. The molar absorption coefficients (ε, $dm^3\,mol^{-1}\,cm^{-1}$) in this region are influenced by the substituent groups of the β-diketonato coligands (Table 1). On the basis of the resonance Raman spectra and the solvent effect as well as the semi-empirical Jørgensen's treatment [32a,35,38,41], these bands are assigned to the metal-to-SOMO (NIT or IM) charge transfer (MLCT) transitions; the metal orbitals being $d_\sigma(e_g)$ and $d_\pi(t_{2g})$ for Ni(II) and Cr(III) complexes, respectively.

For the Ni(II) and Cr(III) NIT2py or IM2py complexes, the band intensities in the spin-forbidden transition are significantly enhanced when compared with those of the corresponding non-radical complexes as shown in Figs. 1 and 2 and Table 1. The large difference in $\varepsilon_{SF}(NIT) = 111–465$ versus $\varepsilon_{SF}(IM2py) = 4.86–11.6$ reflects the antiferromagnetic and ferromagnetic interaction for the NIT2py and IM2py Ni(II) complexes, respectively. Such intensity enhancement can be

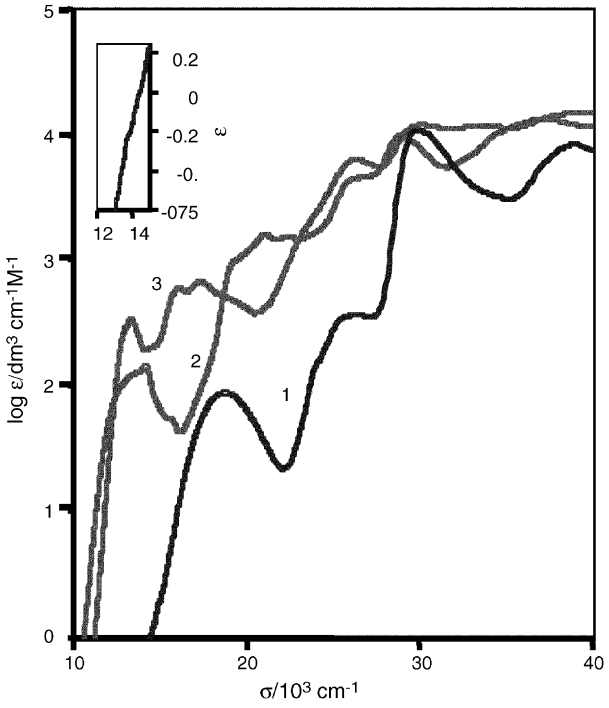

Fig. 1. UV–vis spectra of (1) $[Cr(acac)_2(en)]^+$; (2) $[Cr(acac)_2(IM2py)]^+$; (3) $[Cr(acac)_2(NIT2py)]^+$. *Inset*: The spin-forbidden band of $[Cr(acac)_2(en)]^+$ in CH_2Cl_2 at room temperature.

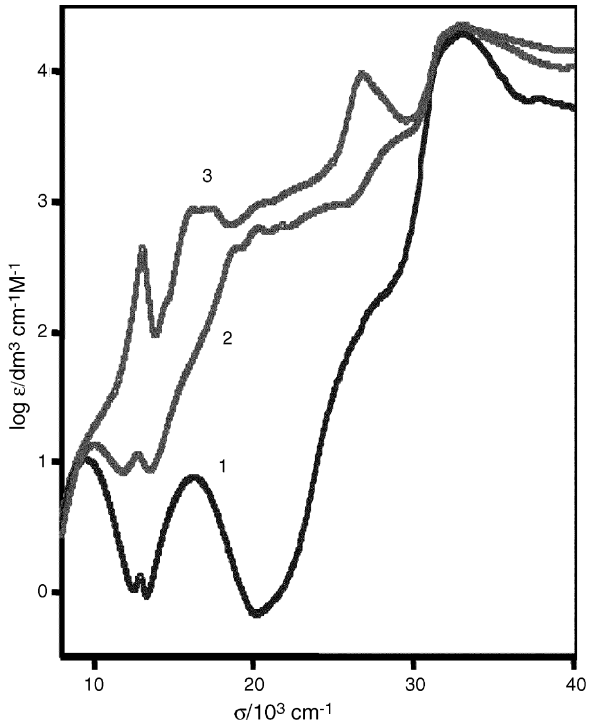

Fig. 2. UV–vis spectra of (1) $[Ni(acac)_2(tmen)]$; (2) $[Ni(acac)_2(IM2py)]$; (3) $[Ni(acac)_2(NIT2py)]$ in CH_2Cl_2 at room temperature.

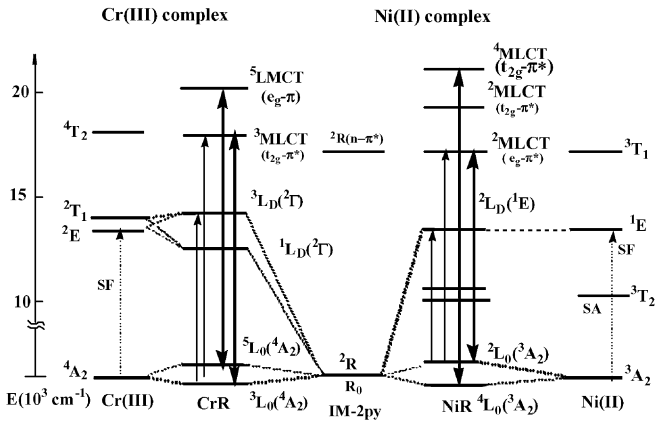

Fig. 3. Energy levels of the nitroxide radical Cr(III) and Ni(II) complexes together with the non-radical complexes.

understood in terms of the exchange interaction between Ni(II) or Cr(III) ion and the NIT2py or IM2py radical as discussed for semiquinone Cr(III) complexes by Benelli et al. [16]. The exchange coupling in the $^3A_2{}^2L_0$(Ni) or $^4A_2{}^2L_0$ (Cr) ground state gives the doublet and quartet or triplet and quintet, whereas only the doublet or the singlet and triplet are generated in the excited state $^2(^1E^2L_0)$ or $^{1\ \text{or}\ 3}(^2E/^2T_1{}^2L_0)$ as shown in Fig. 3. Therefore, the spin-forbidden $^2(^3A_2{}^2L_0) \rightarrow {}^2(^1E^2L_0)$(Ni) or $^3(^4A_2{}^2L_0) \rightarrow {}^3(^2E/^2T_1{}^2L_0)$ transition becomes formally spin-forbidden or actually doublet–doublet or triplet–triplet spin-allowed with the breakdown of the $\Delta S = 0$ restriction. As a result, both transitions borrow intensity from the doublet or triplet MLCT through the admixture of the respective MLCT states into the $^2(^1E^2L_0)$(Ni) or $^3(^2E/^2T_1{}^2L_0)$ states via the electron transfer integral, $h(\mathrm{CT}) = \langle e_g|h|\ \text{SOMO}\ \pi^*\rangle$ for Ni or $\langle t_{2g}|h|\ \text{SOMO}\ \pi^*\rangle$ for Cr. The molar absorption coefficient for the spin-forbidden transition ε_{SF} is formulated approximately as $\{h(\mathrm{CT})/\Delta E_{CT}\}^2\varepsilon_{CT}$, where ε_{CT} is the molar absorption coefficient for the MLCT and ΔE_{CT} is the transition energy difference between the spin-forbidden and MLCT. The variable temperature measurements substantiate this assignment: the intensity enhancement and diminution for the NIT2py Ni(II) and the IM2py Ni(II) complexes, respectively, is in accordance with the antiferromagnetic and ferromagnetic interaction. The similar intensity enhancement with decrease of temperature was observed for the NIT2py and IM2py Cr(III) complexes as shown in Fig. 4, where the inset shows the observed relative intensity and the Boltzmann population calculated with $J = -61.6\,\mathrm{cm}^{-1}$ for $[Cr(acac)_2(NIT2py)]^+$.

The differences in the magnetic and optical properties among the Cr^{III} and Ni^{II} complexes with various β-diketonates were examined in terms of the exchange mechanism [32a,35,38,41]. The constant contribution to the antiferromagnetic coupling constant J_{AF} is approximately expressed as $h(\mathrm{CT})^2/E_{CT}$ or $(\varepsilon_{SF}/\varepsilon_{CT})(\Delta E_{CT})^2/E_{CT}$, where E_{CT} is the transition energy of MLCT and the others were described above. This is derived from the combination between the above-mentioned intensity borrowing mechanism and the configuration interaction between the ground level and the MLCT with the same spin multiplicity (Fig. 3) [32a]. The $(\varepsilon_{SF}/\varepsilon_{CT})(\Delta E_{CT})^2/E_{CT}$ values or J_{ANT} thus estimated

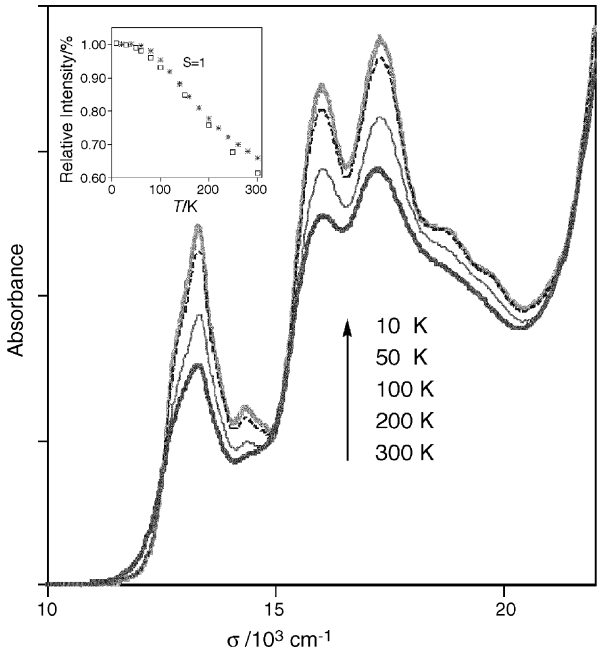

Fig. 4. Variable temperature UV–vis spectra of $[Cr(acac)_2(en)]^+$ in cellulose acetate film. *Inset*: The relative intensity (□) vs. the Boltzmann population (✱) of the triplet ground state calculated with $J = -61.6\,\mathrm{cm}^{-1}$.

for the NIT2py Ni(II) complexes are roughly proportional to the observed J_{obs} as in Table 1. On the other hand, the J_{ANT} for the NIT2py or IM2py Cr(III) complexes and IM2py Ni(II) complexes are almost constant with variation of β-diketonate. Thus, J_{obsd} changes with J_F (Table 1), because of $J_{obsd} = J_{ANT} + J_F$ (vide infra). That is, the ferromagnetic contribution J_F is susceptible to the coligand effect in contrast to the antiferromagnetic one J_{ANT}; according to the argument for the lowest excited state magnetic interaction discussed in Section 2.1.4. This situation accounts for why the difference ε_{SF}(NIT2py) = 230–350 versus ε_{SF}(IM2py) = 150–200 for the Cr^{III} complexes is in contrast to the intuitive prediction from the difference in the magnetic interaction, $|J_{obs}(\mathrm{NIT})| < |J_{obs}(\mathrm{IM})|$. In other words, even though the J_{obs} values for the acacMe complex are smaller by one-tenth than the dpm complex, the degree of intensity enhancement could differ only by 1.4 times (Table 1). This point is important to compare with the monodentate pyridyl coordinating NIT*n*py or IM*n*py Cr^{III} complexes as mentioned below.

2.1.3. *Monodentate IMnpy and NITnpy complexes*

There are inherently weak magnetic interactions and an absence of the intensity enhancement of the spin-forbidden d–d transition bands in the monodentate pyridyl coordinating NIT3py or NIT4py or IM3py or IM4py complexes; this is in contrast to our previous results for the chelated NIT2py and IM2py complexes. This may be accounted for by the difference in the magnetic interaction mechanism [39]. The signs of the magnetic interaction for the NIT*n*py and IM*n*py complexes change alternatively with the intervening atoms between the Cr^{III} and the radical moiety in the π-electron system including the nitroxide π^* and Cr^{III} dπ orbitals just as predicted by a spin-polarization mechanism (Scheme 2).

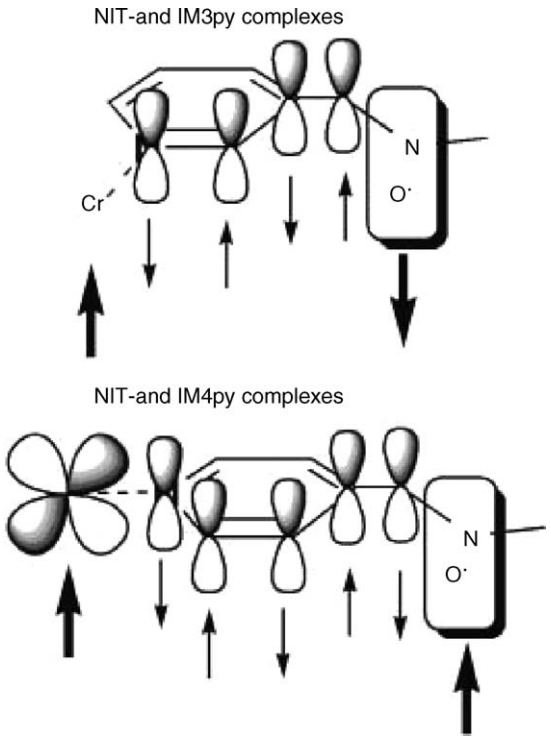

Scheme 2.

This is evidently substantiated by the fact that ferro- and antiferromagnetic interactions were found, respectively, for the 3- and 4-(*N*-oxy-*N*-*tert*-butylamino)pyridine (*n*NOpy; $n = 3$ or 4) Cr^{III} complexes [Cr(TPP or TAP)Cl(*n*NOpy)] {TPP = *meso*-tetraphenylporphyrinate(2–), TAP = *meso*-tetrakis(methoxyphenyl)porphyrinate(2–)} [45]. That is, the positive and negative signs of J for the 3NOpy and 4NOpy complexes are opposite to those of the NIT3py and 4py or IM3py and 4py Cr^{III} complexes. Moreover, the magnitude of J for the NIT*n*py or IM*n*py complexes ($|J| = 2$–$6\,cm^{-1}$) are an order of magnitude smaller than those of the 3NOpy or 4NOpy complexes. Such opposite signs and diminution in magnitude of J may be due to one extra intervening bond in 4py or 3py. This leads to the different phase of π electron spin-polarization in the pyridine and the difference in magnitude due to a node at the carbon between the two nitrogen atoms of NIT or IM. Assuming that the spin-polarization mechanism operates for the NIT2py and IM2py complexes, ferromagnetic interactions are predicted through the pyridyl nitrogen. However, this is not what is found; only antiferromagnetic interactions are observed as mentioned above. Other than the J_{ANT} or $(\varepsilon_{SF}/\varepsilon_{CT})(\Delta E_{CT})^2/E_{CT}$ estimated from the spectroscopic data, it is seen that the ferromagnetic interaction, J_F, exhibiting the coligand effect(vide supra) includes another ferromagnetic interaction due to the spin-polarization mechanism. On the other hand, the magnetic interaction for the NIT*n*py and IM*n*py Cr^{III} complexes ($n = 3$ or 4) would predominantly originate from the spin-polarization mechanism; i.e., $J_{obs} = J_{ANT}$ for the NIT3py and IM3py or $J_{obs} = J_F$ for the NIT4py and IM4py complexes.

In contrast to the large intensity enhancement of the spin-forbidden d–d transitions for the NIT2py and IM2py Cr^{III} complexes, the monodentate NIT*n*py and IM*n*py Cr^{III} complexes show no enhancement. This is not necessarily due to the small magnitude of J_{obs} as compared with those for the NIT2py and IM2py complexes. By considering the exchange mechanism for the magnetic interactions, however, it follows that a large magnitude of J_{obs} is both required and sufficient for the intensity enhancements, but that the reverse is not true; even for the diminution of J_{obs}, the intensity is enhanced as expected from the constant contribution of J_{ANT}, irrespective of a large variation of the J_{obs} values for the NIT2py and IM2py Cr^{III} complexes. That is, a sufficient condition for the intensity enhancement is not a large magnitude of J_{obs}, but rather the appearance of the MLCT bands due to the large overlap between the SOMO π^* and the dπ orbitals that augments the J_{ANT} values in terms of the exchange mechanism. Thus no observation of the spin-forbidden transition intensity enhancement for the indirect pyridyl coordinating NIT*n*py and IM*n*py complexes arises from the absence of the dπ–SOMO MLCT or no overlap of the d orbital with the SOMO of NIT or IM radical, but not necessarily from the small J_{obs} magnitude as mentioned above.

2.1.4. The lowest excited ligand field state of the Cr(III) complexes

The magnetic interactions in the lowest excited states are important to understand the electronic structure and to explore the photochemistry and photophysics of the spin-coupled systems. There have been several studies of metal–metal dimers by the combined measurements of the absorption and emission spectra [1,46], but none for radical complexes. This is the first observation of the lowest excited state magnetic interaction [42].

For the NIT2py and IM2py Cr(III) complexes, the fairly sharp luminescence band appears at about 12,000 and 9500 cm^{-1}, respectively (Fig. 5). These luminescence bands are displaced to lower energy by 1500 and 4340 cm^{-1}, respectively, from the lowest energy absorption and MCD bands, which are due to the formally spin-forbidden $^3L_0(^4A_2) \rightarrow {}^3L_D(^2\Gamma)$ transitions between the spin-coupled states originating from the $^4A \rightarrow {}^2\Gamma(^2E,{}^2T_1)$ d–d transitions (Figs. 5 and 6). There are three possible causes for these emission features: (i) intraligand (ligand centered) luminescence from the SOMO π^* to the *n*(HOMO) orbital in the NIT2py or IM2py radical; (ii) $^3L_D(^2\Gamma) \rightarrow {}^3L_0(^4A_2)$ d–d fluorescence; (iii) $^1L_D(^2\Gamma) \rightarrow {}^3L_0(^4A_2)$ phosphorescence. It is seen from the following that the former cases (i) and (ii) are ruled out and that the case (iii) is valid. The luminescence of the NIT2py complex does not originate from a radical intraligand transition, because this is qualitatively different from the intraligand luminescence observed for the 4f–4f non-emissive radical lanthanide complex $[Lu^{III}(hfac)_3(NIT2py)]$ as shown in Fig. 7. As compared with the Stokes shifts [47] for the inter-subshell (e_g–t_{2g}) fluorescence from $^4T_{2g}$ to $^4A_{2g}$ of the Cr(III) complexes, these "shifts" (1500–4340 cm^{-1}) are too large for the $^3L_D(^2\Gamma) \rightarrow {}^3L_0(^4A_2)$ spin-flip intra-subshell (t_{2g}–t_{2g}) luminescence at the metal center. This is true even in view of a possible mixing with the MLCT and a mirror image correlation between the absorption and the

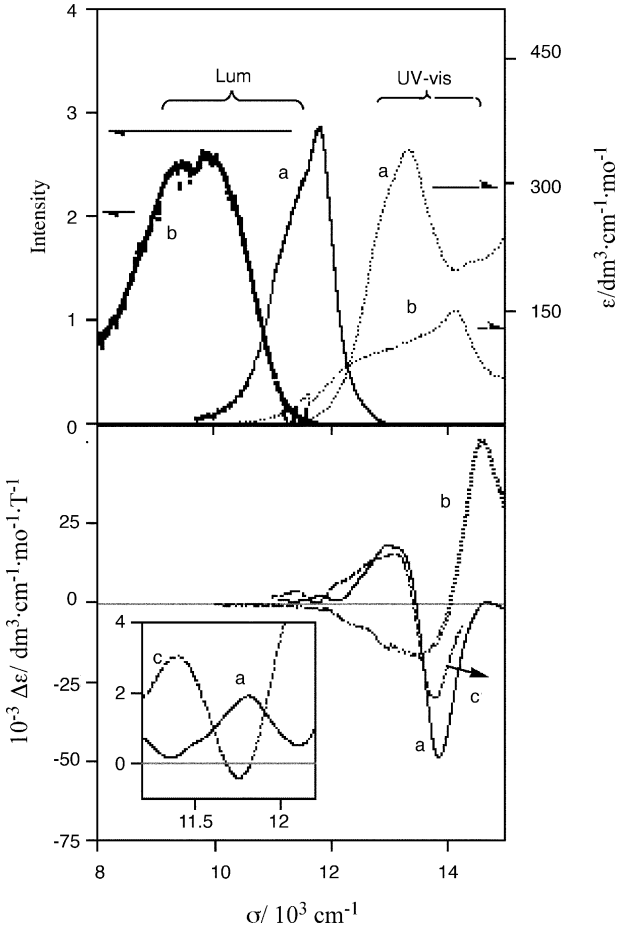

Fig. 5. *Top*: UV–vis absorption spectra in CH_3CN at 300 K and luminescence spectra in solid state at 15 K of $[Cr(acac)_2(NIT2py)]PF_6$ (a) and $[Cr(acac)_2(IM2py)]PF_6$ (b). *Bottom*: MCD spectra of $[Cr(acac)_2(NIT2py)]PF_6$ (a), $[Cr(acac)_2(IM2py)]PF_6$ (b) and $[Cr(bzac)_2(NIT2py)]PF_6$ (c) in CH_3CN at 300 K (adapted from ref. [42]).

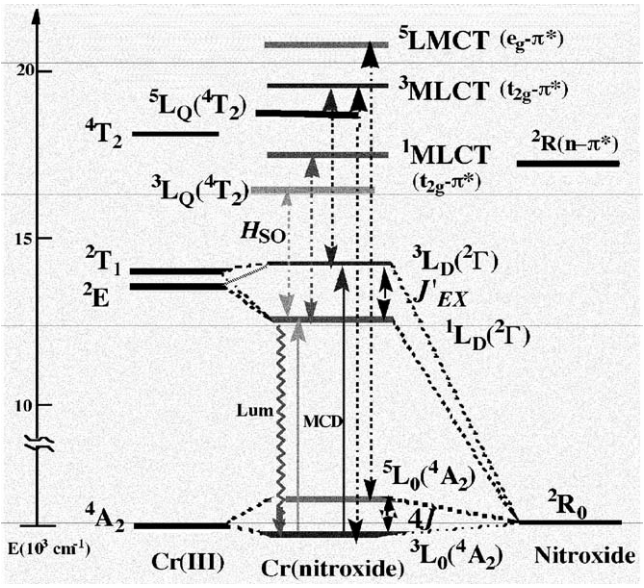

Fig. 6. Energy levels of nitroxide radical Cr(III) complexes (center) together with non-radical Cr(III) complexes (left) and nitroxide itself (right). Thick solid vertical lines and a wavy vertical line indicate MCD and luminescence, respectively. Dotted vertical lines show the configurational interactions (CI) between the ground and the excited states and/or MLCT states with the same spin multiplicity (adapted from ref. [42]).

corresponding luminescence spectra. On the other hand, a much weaker and narrower positive MCD band of the NIT2py complex at $11.80 \times 10^3\ cm^{-1}$ is located near the luminescence band with half band width similar to those of the deconvoluted components of the main luminescence band as shown in Fig. 5. Accordingly, it is plausible that the luminescence arises from the intrinsic spin-forbidden $^1L_D(^2\Gamma) \rightarrow {}^3L_0(^4A_2)$ transition (Figs. 6 and 7). For the IM2py Cr(III) complex, the luminescence is also quite different from that of the IM2py Lu(III) complex, though the corresponding MCD could not be observed owing to instrumental limitations. Similar results for two series of β-diketonate complexes are obtained among absorption and/or MCD and luminescence patterns (Fig. 5; Table 1).

The energy gaps between the singlet and triplet levels or the magnetic interaction in the lowest excited state are estimated to be much larger than those ($4J$) in the ground state (Table 1). This is in accordance with the generally observed enlargement of the magnetic interactions for the excited states as compared with the ground state in exchange coupled systems of metal–metal dimers [1,46]. The increase of magnetic interactions in the excited state is much larger than that found for the metal–metal dimers. Such an increase in magnetic interaction is associated not only with increasing electron transfer character in the excited states [1,46,48,49], but also with the lower energy of the ^{3}MLCT and ^{1}MLCT in the NIT2py and IM2py complexes compared with the LMCT or MMCT states in the metal–metal dinuclear complexes [1,46,48,49]. This results in larger configurational interaction (CI) among the excited states (Fig. 7), which increases the energy gap in the first lowest excited state.

The excited state magnetic interactions are found to vary from 1500 to 2000 cm^{-1} and from 3600 to 4400 cm^{-1}, in the

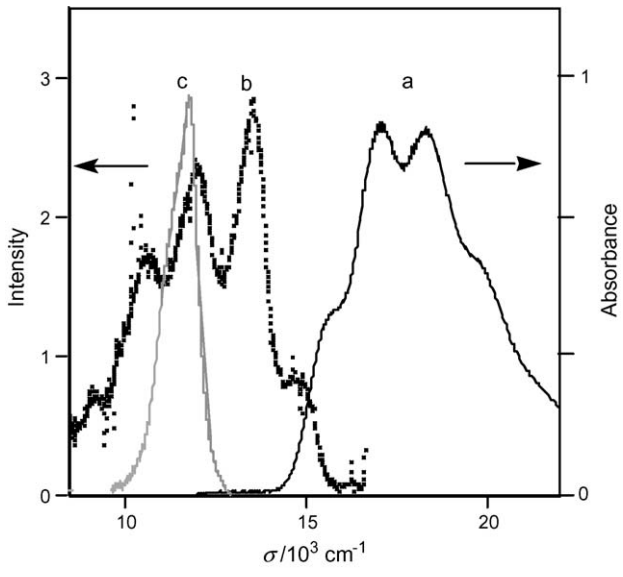

Fig. 7. UV–vis absorption spectra (a) in CH_2Cl_2 at 180 K and luminescence spectra and (b) in solid state at 15 K of $[Lu(hfac)_3(NIT2py)]$. Luminescence spectra (c) in solid state at 15 K of $[Cr(acac)_2(NIT2py)]PF_6$ (adapted from ref. [42]).

NIT2py and IM2py complexes, respectively. Notably, these variations are much smaller than the ground state values (Table 1). As discussed according to the VBCI model in Section 2.1.2, the configurational interaction between $^1L_D(^2\Gamma)$ and ^{1}MLCT or $^3L_D(^2\Gamma)$ and ^{3}MLCT depends upon the integral $\langle t_{2g}|h|$SOMO $\pi^*\rangle$ or the orbital overlap, $\langle t_{2g}||$SOMO $\pi^*\rangle$, between the t_{2g} and π^* orbitals which exert no coligand effect. However, the CI between the ^{5}LMCT and $^5L_Q(^4A_2)$ depends upon $\langle e_g||$HOMO $\pi\rangle$, which is why the ferromagnetic interaction is affected by the coligand effect (Fig. 7) as mentioned in Section 2.1.2.

These results give important insight into the effect of the coordination of the nitroxide radicals on the excited states with respect to their photochemistry.

2.2. Diamagnetic Co(III) complexes

Though there is no magnetic interaction in the ground state owing to the diamagnetic low spin Co(III) complexes, it is intriguing to see whether the lowest excited triplet state of Co(III) complexes is influenced by coordinated NIT or IM radicals. This is the reverse situation from the magnetic interaction between the triplet state in diamagnetic ligands and nearby paramagnetic species such as central metal ions [26,27] or dissolved dioxygen molecule [50] as mentioned in the following section. According to the above theoretical consideration, however, little or no intensity enhancement of the singlet–triplet d–d transitions is predicted even for the chelated Co^{III} (NIT2py or IM2py) complexes, since the electron transfer integral between the ligand field $^3T_1(t_{2g}{}^5e_g{}^1)$ and $^3T_2(t_{2g}{}^5e_g{}^1)$ states and the SOMO, $h^{Co}_{e\pi^*} = \langle|e_g^+|h|$SOMO $\pi^*|\rangle$, or the overlap between the $e_g(d_\sigma)$ and π orbitals would be negligibly small. We attempted to synthesize $[Co^{III}(trien)(NIT2py)]^{3+}$ (trien = trimethylenetetramine) from $[Co^{III}(trien)(CF_3SO_3)_2](CF_3SO_3)$ with NIT2py or Na-$[Co^{III}(acac)_2(IM2py)]$ from *trans*-$Na[Co(NO_2)_2(acac)_2]$ with IM2py. However, this has failed so far but resulted in forming the reduced Co(II) complex *trans*-$[Co^{II}(NIT2py)_2(H_2O)_2](CF_3SO_3)_2$ [51] or one-electron reduced imino nitroxide complex *trans*-$[Co(NO_2)_2(acac)(IMH2py)]$(IMH2py = 1-hydroxyl-2(2′-pyridyl)-4,4,5,5-tetramethyl-4,5-dihydro-1H-imidazole) [52], respectively.

2.3. Co(II) complexes

Magnetic interactions for high-spin Co(II) complexes where there is a magnetic orbital in both the t_{2g} and e_g subshells are examined to demonstrate the difference from those for Ni(II) and Cr(III) complexes which have magnetic orbitals either in the t_{2g} or e_g subshells. For four complexes of $[Co(Rtfac)_2(IM2py)]$ (Rtfac = hfac, bztfc, thtfc, natfc), the magnetic exchange interactions or J values between Co(II) and IM2py vary with the β-diketonate coligands. The hfac complex exhibits the fairly large positive J value (+21 cm^{-1}) or ferromagnetic interaction, whereas smaller J values are found, a very weak antiferromagnetic (−0.87 cm^{-1}) for the bztfc complex or weaker ferromagnetic (+3.14 and +4.47 cm^{-1}) interactions, respectively, for the thtfc and natfc complexes as estimated from least squared fits of the variable temperature magnetic susceptibility measurements (Fig. 8). Such magnetic behavior may be correlated to the d orbital energy splitting.

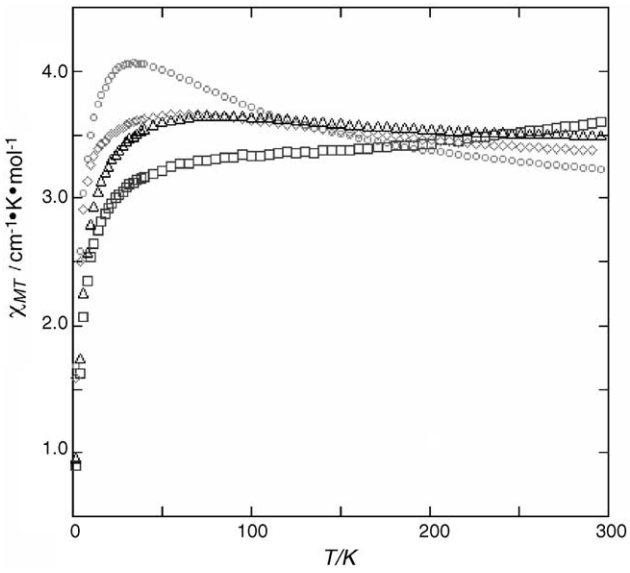

Fig. 8. Plots of $\chi_M T$ vs. T of [Co(β-diketonato)$_2$(IM2py)]: (◯) hfac; (□) bztfc; (◇) natfc; (△) thtfc.

The difference in magnetic properties originates from two interactive modes between unpaired electrons in Co(II) ion and IM2py. They are the interactions $J_{d\sigma}$ and $J_{d\pi}$, respectively, between the $d_\pi(t_{2g})$ or $d_\sigma(e_g)$ orbitals in the cobalt(II) ion and the SOMO in IM2py. Since the plane (N–C–N–O) of the radical moiety in IM2py and the coordination plane (N(IM)–Co–N(py)) are almost coplanar to each other, the d_σ orbitals of cobalt(II) ion are orthogonal to the SOMO of the IM2py, thus the magnetic interaction of IM2py with the d_σ could be ferromagnetic ($J_{d\sigma} > 0$) as with the Ni(II) complexes. On the other hand, there are two possibilities for the interactions between the d_π orbital and the SOMO, depending on the splitting patterns of the d_π orbitals as discussed for *cis*-$[CoCl_2(IM2py)]$ in terms of the Angular Overlap Model (AOM) [33]. One case is the overlap of the magnetic d_π orbital having an unpaired electron with the SOMO. In this case, the magnetic interaction is antiferromagnetic ($J_{d\pi} < 0$) as seen for Cr(III) complexes. The other case is the orthogonality of the magnetic d_π orbital with the SOMO, where the magnetic interaction between the SOMO and the d_π orbital is ferromagnetic ($J_{d\pi} > 0$). The total or observed coupling constant J (J_{obs}) is represented by $J_{obs} = J_{d\sigma} + J_{d\pi} = 1/3\{J_{F(d\sigma)} + J_{F(d\sigma)} + J_{ANT(d\pi)}\}$ or $1/3\{J_{F(d\sigma)} + J_{F(d\sigma)} + J_{F(d\pi)}\}$.

The coligand effect of the β-diketonate on the magnetic properties originates from the different d_π orbital splitting pattern. The d_π orbital energies are expressed by the AOM parameters as follows:

$$\varepsilon(d_{zx}) = e_\pi(N(IM)) + e_\pi(O(CF_3)),\ \varepsilon(d_{xy}) = 2e_\pi(O(R)),$$
$$\text{and } \varepsilon(d_{yz}) = e_\pi(N(py)) + e_\pi(O(CF_3))$$

where $e_\pi(O(R))$, $e_\pi(O(CF_3))$, $e_\pi(N(IM))$ and $e_\pi(N(py))$ are the AOM parameters, which represent the interaction energy

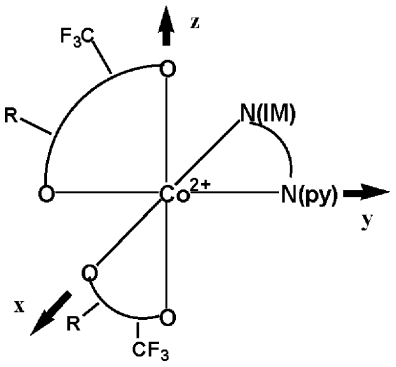

Scheme 3.

between the π orbital of the donor ligand atoms and the d_π orbital orthogonal to the chelate planes: O(R) and O(CF_3) being O(O–C–R) and O(O–C–CF), respectively, in Rtfac: N(IM) and N(py) being N (N = C–N–O) and N(pyridyl), respectively, in IM2py. The coordinate of the donor atoms in these complexes is depicted in Scheme 3 with the *trans*-(CF_3) geometrical structures which were demonstrated by the X-ray analysis.

There are two cases (a) and (b) for the energy level order on the assumption of transferability of the e_π(N(IM)), e_π(N(py)) and e_π(O(CF_3)) through a series of these complexes, negative or small positive e_π(N(py)) due to the acceptor or weak donor pyridyl group, and positive e_π(N(IM)) due to the donor imidazole. For both cases, the d_{yz} is supposed to be the lowest orbital owing to the π acceptor pyridyl group, $e_\pi(\mathrm{N(py)}) < 0$ [54].

$$\varepsilon(d_{zx}) > \varepsilon(d_{xy}) > \varepsilon(d_{yz}) \quad \text{(a)}$$

$$\varepsilon(d_{xy}) > \varepsilon(d_{zx}) > \varepsilon(d_{yz}) \quad \text{(b)}$$

In case (a), the highest occupied magnetic d_π orbital with an unpaired electron is d_{zx}, which could overlap with the SOMO, leading to antiferromagnetic interaction. Thus, the total magnetic interaction or a sum of the $J_{F(d\sigma)}$ and $J_{ANT(d\pi)}$ would become smaller as a result of cancellation between the ferromagnetic and the antiferromagnetic interactions. This accords with the small antiferromagnetic or ferromagnetic interaction as observed for the bztfc, thtfc and natfc complexes. On the other hand, in case (b) where the magnetic d_π orbital with an unpaired electron is the d_{xy}, orthogonality with the SOMO results in a ferromagnetic interaction. Then both contributions to the magnetic interaction from the d_σ and d_π are ferromagnetic, so that there may be a fairly large ferromagnetic interaction as observed for the hfac complex. Then, this energy level order could result from the difference in the electronic properties between the electron withdrawing CF_3 and the electron donating R groups. From the viewpoint of AOM parametrization, the energy difference $\Delta\varepsilon = \varepsilon(d_{xy}) - \varepsilon(d_{zx}) = 2e_\pi(\mathrm{O(R)}) - (e_\pi(\mathrm{N(IM)}) + e_\pi(\mathrm{O(CF_3)}))$ is negative and positive for cases (a) and (b), respectively. This results in $e_\pi(\mathrm{O(CF_3)}) > e_\pi(\mathrm{N(IM)})$ for the hfac complex and $2e_\pi(\mathrm{O(R)}) < e_\pi(\mathrm{N(IM)}) + e_\pi(\mathrm{O(CF_3)})$ or $e_\pi(\mathrm{O(R)}) < e_\pi(\mathrm{O(CF_3)})$ for the other Rtfac complexes being estimated. The relationship $e_\pi(\mathrm{O(R)}) < e_\pi(\mathrm{O(CF_3)})$ is plausible, since the destabilization of the d electrons by the CF_3 group for the hfac complexes is inferred from the charge transfer spectra

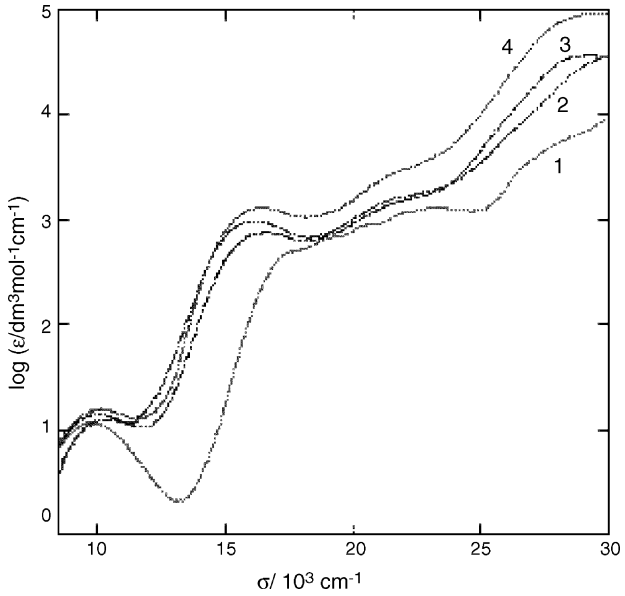

Fig. 9. UV–vis spectra of [Co(β-diketonato)$_2$(IM2py)]: (1) hfac; (2) thtfc; (3) bztfc; (4) natfc.

of the β-diketonato Cr(III) complexes [55]. Thus, the difference in the d orbital energy level or magnetic interaction results from the change of the electronic properties or AOM parameters with variation of the β-diketonates.

There is also found to be large differences in the position of the intense broad visible bands or shoulder from 15,000 to 25,000 cm^{-1} between the three Rtfac (bztfc, thtfc and naphtfc) complexes and the hfac complex; the former around 16,500 and 20,000 cm^{-1} and the latter at 17,500 and 24,000 cm^{-1}, apart from the first spin-allowed d–d $^4T_1 \rightarrow {}^4T_2$ absorption band around 10,000 cm^{-1} as in Fig. 9. On the basis of the resonance Raman spectra and the solvent effect in this region or Jørgensen's semi-empirical treatment [56], the band or shoulder around 16,000–17,500 cm^{-1} is assigned to the $e_g \rightarrow$ SOMO MLCT. The higher frequency band around 20,000–24,000 cm^{-1} may be due to the $t_{2g} \rightarrow$ SOMO MLCT. These assignments are supported by the similarity of MCD pattern as shown in Fig. 10. Both the Rtfac and hfac complexes give weak and strong positive MCD peaks with the transition energy differences of 500 and 2800 cm^{-1}, respectively, from the longer wavelength side. This shift tendency for the hfac complex may be due to the following causes, though the magnitudes of the shifts are much smaller than the predicted ones. The small blue shift of the e_g SOMO MLCT would result from the decrease by about 120 cm^{-1} in the ligand field splitting Δ, as seen from the UV–vis spectra in Fig. 9. The much higher frequency shift of the $t_{2g} \rightarrow$ SOMO MLCT may arise from the difference in spin-pairing energy for the transition from $(d_{yz})^2(d_{zx})^2(d_{xy})^+(d_{z2})^+(d_{x2-y2})^+(\mathrm{SOMO})^-$ to $(d_{yz})^2(d_{zx})^-(d_{xy})^+(d_{z2})^+(d_{x2-y2})^+(\mathrm{SOMO})^2$ for the hfac complex when compared with that from $(d_{yz})^2(d_{xy})^2(d_{xz})^+(d_{z2})^+(d_{x2-y2})^+(\mathrm{SOMO})^-$ to $(d_{yz})^2(d_{xy})^2(d_{z2})^+(d_{x2-y2})^+(\mathrm{SOMO})^2$ (vide supra).

Consequently, the magneto-optical properties of the present β-diketonato IM2py Co(II) complexes or the ferromagnetic interaction and the higher energy shift of the MLCT for the

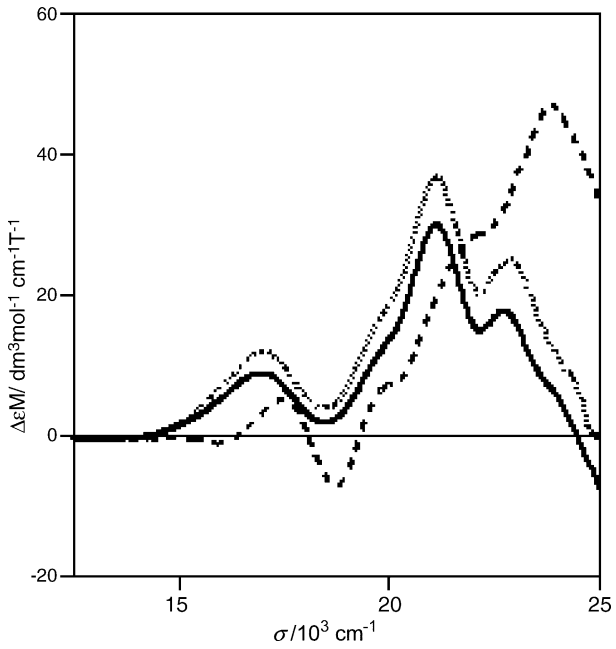

Fig. 10. MCD spectra of [Co(β-diketonato)$_2$(IM2py)]: thfc (dotted line); bzfc (solid line); hfac (broken line).

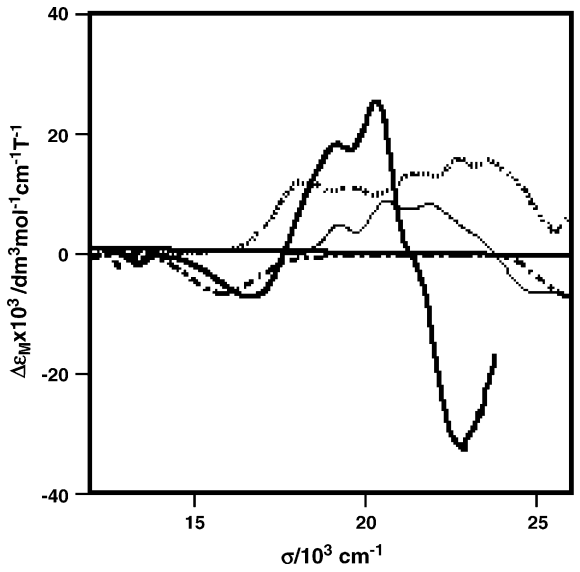

Fig. 11. MCD of IM2py ($\Delta\varepsilon_M \times 2$) (. . . . .), [Ni(acac)$_2$(tmen)] (- - - -), [Ni(IM2py)(H$_2$O)$_4$]SO$_4$·0.5H$_2$O (—) and [Ni(acac)$_2$(IM2py)] (▬) in CH$_3$CN at room temperature.

hfac complex can be accounted for by the AOM parametrization and/or the ligand field and the interelectronic repulsion parameters. These parameters vary with the change of electronic properties on going from CF_3 to the R groups with the specific topological disposition in the *trans*-(CF_3) isomeric structure. Accordingly, this fact suggests the possibility to regulate magneto-optical properties by changing the electronic properties of the substituents in the β-diketonate coligand as mentioned in Section 2.1 for the Ni(II) and Cr(III) complexes.

3. Intraligand transitions

3.1. The singlet–triplet transition of ancillary acetylacetonate ligands

As mentioned above, it has been reported that the singlet–triplet (S–T) transition intensity in diamagnetic organic ligands (e.g., aromatic imines or acetylacetonate) is enhanced in the presence of paramagnetic Cr(III) complexes [26,27]. This is also observed in pyridine under perturbation of dissolved paramagnetic dioxygen molecule [50]. This is analogous, in an inverted sense, to the intensity enhancement of the singlet–triplet transition in diamagnetic moieties such as the lowest excited triplet state of diamagnetic Co(III) complexes with the nitroxide radicals (vide supra). In the coordinated acetylacetonates or aromatic imines such as 2,2′-bipyridine in Cr(III) complexes, the intraligand S–T transition (^{4}(^{3}LE)) intensities are found to be intensified through borrowing the singlet-singlet π–π* transition (^{4}(^{1}LE)) intensity via the ^{4}(MLCT(Cr-to-acac)) with the same spin multiplicity through orbital overlap between the t_{2g} and π orbitals. This was verified through luminescence and MCD spectra and also semi-quantitative theoretical consideration [27].

As shown in Fig. 11, [Ni(acac)$_2$(IM2py)] complex gives a negative strong MCD band around 22.5×10^3 cm^{-1} together with lower frequency positive MCD components probably due to the intraligand n-SOMO π* transition of IM2py. This is compared with the positive vibronic MCD peaks of [Ni(IM2py)(H$_2$O)$_4$](SO$_4$) and with the relatively weaker negative MCD around 27×10^3 cm^{-1} due to the third d–d ^{3}A$_2$–^{3}T$_1$ transition of [Ni(acac)$_2$(tmen)]. On the other hand, in the region near 22.5×10^3 cm^{-1}, there is no negative MCD for [Ni(IM2py)(H$_2$O)$_4$](SO$_4$) and [Ni(acac)$_2$(tmen)] (Fig. 11). Therefore, it is suggested that the negative component at 22.5×10^3 cm^{-1} for [Ni(acac)$_2$(IM2py)] is not due either to the intraligand transition in IM2py nor to the negative d–d MCD band. No observation of the S–T transition of the non-radical complex [Ni(acac)$_2$(tmen)] could result from the orthogonality between the π orbital of the β-diketonato ligand and e$_g$ orbital of the Ni(II) ion in contrast to the case of the Cr(III) complexes where there is the overlap between the t_{2g}(Cr(III)) and π(acac) orbitals [27]. Therefore, the S–T transition intensity cannot borrow from the singlet-singlet π–π* transition of the acac through the MLCT (Fig. 12). Only the IM2py Ni(II) acac complexes exhibited intensity enhancements in the intraligand spin-forbidden ^{1}LE → ^{3}LE (S–T) acetylacetonate transition. Thus, this arises from the combination between the IM2py SOMO π* and the acetylacetonate π orbital. In other words, the intensity enhancement of the ^{2}L(^{3}LE)-^{2}(^{3}A$_2$) transition could arise through borrowing the singlet–singlet π–π* transition (^{2}(^{1}LE-^{3}A$_2$)-^{2}(^{1}LG-^{3}A$_2$)) intensity of the acetylacetonate through the inter-ligand-to-ligand charge transfer transition (^{2}LLCT) between the IM2py SOMO π* and the ^{1}LE(acac). This is possible since the orbital overlap between π*(IM2py) and π*(^{1}LE) for the LLCT is non-zero as shown in Fig. 12. So far, the LLCT could not be detected in the absorption spectra in the near infrared region probably owing to its weak intensity and poor overlap [58]. It should be possible to observe the LLCT transi-

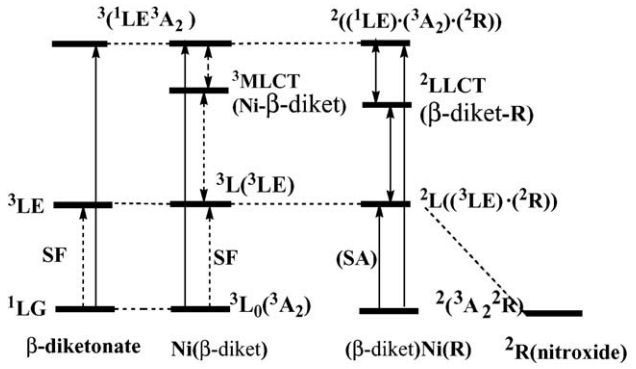

Fig. 12. Energy levels showing the borrowing mechanism of the S–T transition intensity from the π–π* of the acac through MLCT or LLCT of [Ni(acac)$_2$(tmen)] (left) and [Ni(acac)$_2$(IM2py)] (right).

tion in d^{10} metal complexes such as [Zn(acac)$_2$(IM2py)]. The analogous intensity enhancement may be expected in low-spin acac Co(III) complexes with nitroxide radicals again assuming involvement of the LLCT transition.

3.2. Nitroxide radical ligands

3.2.1. Cr(III) and Ni(II) complexes

Another coordination effect of the NIT2py and IM2py ligands is demonstrated in the intraligand $n \rightarrow \pi^*$ and $\pi \rightarrow \pi^*$ transitions which are located, respectively, at 17,500 and 27,200 cm^{-1} for the nitronyl nitroxide (NIT) moiety and at 22,000 and 33,300 cm^{-1} for the imino nitroxide (IM) moiety. As with the ultraviolet spectroscopic characteristics of the Cr^{III}(IM2py) and Ni^{II}(IM2py) complexes, the vibronic structure around 20.0×10^3 cm^{-1} may originate from the intraligand $n \rightarrow \pi^*$ transition, in view of the similarities in intensity and shift behaviors for variation of the β-diketonates as well as for the Ln^{III}(IM2py) complexes [32–42]. These features are also more clearly displayed in the MCD [57]. We have also observed significant influences on the n–π^* and $\pi \rightarrow \pi^*$ absorption bands for the diamagnetic Co(III) and paramagnetic Cr(III) complexes bearing monodentate NIT3py or NIT4py and IM3py or IM4py [36a,39]. Despite giving weaker magnetic interactions between the pyridyl group of the nitroxides and metal ions as mentioned in Section 2.1.3, the red shift for the NIT4py complexes is larger than the NIT3py complexes. These differences in perturbation between the NIT4py and NIT3py complexes may result from the differences in spin density (and sign) at the pyridyl-N atom as found for the ^{59}Co NMR chemical shifts of the NIT4py and NIT3py complexes [36a] and the signs of the magnetic interactions of the corresponding Cr(III) complexes [39]. These perturbed properties may be related to the unusual diamagnetic NMR behavior of the radical ligands in the Co^{III}(IM3py or IM4py) [36b] and Ln^{III}(IM2py) complexes [37d]. Interestingly, we have recently found that the MCD intensities for the intraligand transitions of the nitroxide radical in the Ni(II) complexes are much larger than those in the Lu(III) complex with non-magnetic interaction or in the nitroxide radical ligands themselves (Fig. 11), suggesting also a magnetic interaction between the two magnetic centers [57].

3.2.2. Lanthanide(III) complexes

The intraligand transitions in the nitroxide radicals or their Ln(III) complexes have been studied in relation to the magnetic or photochemical and photophysical behavior of the NIT2py or IM2py Ln(III) complexes [37a,59,60]. When compared with the intraligand n–π^* transition of IM2py in the region from 19×10^3 to 24×10^3 cm^{-1}, the corresponding bands of [Ln(hfac)$_3$(IM2py)] are shifted to lower frequency and have much larger molar absorption coefficients of each vibronic component with more distinct vibrational structure than the uncoordinated IM2py ligand [37a] as observed in [Gd(NITBzIMH)$_2$(NO$_3$)$_3$] [59,60]. This curious behavior may arise either from chelation which slightly stabilizes the radical SOMO π^* energy level due to increase in planarity between N=C–N=O moiety and pyridine ring, or from the coordinate bond with lanthanide(III) ion which considerably affects the electronic state of the ligand, as also observed for Schiff base complexes [61]. These features of the intraligand transition of the nitroxide radicals are more clearly demonstrated by the variable temperature MCD measurements of [Lu(hfac)$_3$(IM2py)]. This complex shows a few vibronic positive peaks with a weak longer wavelength negative component and increase in intensity with lowering the temperature, giving the C term of MCD [57]. It is interesting to compare the above results with the recent study by Reber, Luneau and co-workers [59,60] who claimed two components for the UV–vis spectra in the intraligand nitroxide transition region. They postulated that both the energy difference between the ground and low-energy excited states and the detailed band shape of the luminescence spectra are qualitatively correlated with the ferromagnetic or antiferromagnetic interaction in nitroxide radical Ln(III) complexes.

4. Luminescence of lanthanide(III) complexes

Much attention has been paid to near infrared (NIR) luminescence of lanthanide(III) complexes with aromatic imines or organic dyes from a viewpoint of low cost NIR light sources for communications or sensing and biological applications [62–64]. When compared with these cases, radical lanthanide complexes could have intriguing emitting properties in view of difference in spin multiplicity of ligand excited state on going from triplet (organic substances) to doublet (radicals). Luneau, Reber and co-workers reported the visible luminescence spectra of the uncoordinated and coordinated nitroxides [59,60], while the NIR emission spectra of the Ln(III)–Cr(III) dinuclear complexes afforded information on the energy transfer from the Cr(III) $^2E/^2T_1$ state to the 4f state [65].

In this section, the luminescence in solid state are examined for [Ln^{III}(hfac)$_3$(NIT2py)] from a view point of the energy transfer or antenna effect.

Since the band contours with vibronic structure of absorption and luminescence spectra of non-4f–4f-emissive Lu(III) complex show a mirror image relation, the luminescence at $9–15 \times 10^3$ cm^{-1} is the intraligand doublet–doublet (D–D) luminescence from the only one SOMO π^* excited state as shown in Fig. 13, in contrast to the NITBzimH Ln(III) complexes which were claimed to have two SOMO π^* states on the

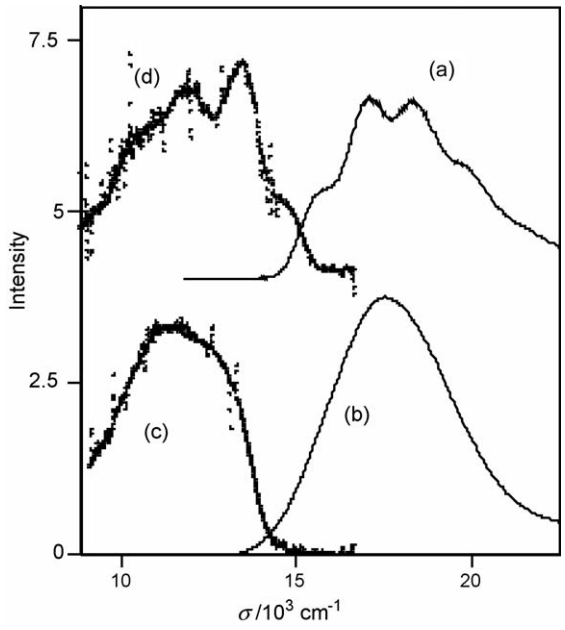

Fig. 13. UV–vis spectra (dotted lines) in CH_2Cl_2 at 180 K and luminescence spectra (solid lines) in solid state at 180 K of Lu(III) complex (a and d) and NIT2py ligand (b and c), respectively (adapted from ref. [44]).

basis of the close comparison between the absorption and luminescence spectra and the DFT calculations by Reber, Lunuea and co-workers [60].

For the vis-emissive Eu(III) and Sm(III) complexes, only the intraligand (D–D) luminescence was observed at 15 K. This results from the energy transfer from the 4f levels to the SOMO π^* level, as compared to the cases of [Eu^{III}(hfac)$_3$(IM2py)] and [Eu^{III}(hfac)$_3$(NITBzImH or IMBzImH)] (NITBzImH or IMBzImH = 2-(2-benzimidazolyl)-4,4,5,5-tetramethyl-4,5-dihydro-1H-imidazolyl-3-oxide-1-oxyl; IMBzImH 2-(2-benzimidazolyl)-4,4,5,5-tetramethyl-4,5-dihydro-1H-imidazol-1-oxy). For [Eu^{III}(hfac)$_3$(IM2py)], the visible 4f–4f luminescence was observed by 222 nm excitation corresponding to the intraligand hfac transition, but not by 465 nm one to the intraligand IM2py transition at room temperature; exhibiting the energy transfer from the triplet state of the ancillary hfac ligand [37a]. However, at 5 K the intraligand (IM2py) luminescence was observed by the Ar^+ laser excitation. The NIT2py Eu(III) complex [Eu^{III}(hfac)$_3$(IM2py)] gives only the intraligand (NIT2py) luminescence, probably due to the lower lying of SOMO π^*(NIT2py) than SOMO π^*(IM2py) as shown in Fig. 14. On the other hand, the luminescence behavior of the [Eu(NITBzImH)$_2$(NO$_3$)$_3$] is similar to that of the present NIT2py complex, whereas [Eu(hfac)$_3$(NITBzImH or IMBzImH)] demonstrate both the intraligand and visible 4f–4f luminescence [59,60]. This difference results from the relative location between the SOMO π^* band envelope of nitroxide radicals and the emissive 4f energy levels as in Fig. 14.

As shown in Fig. 15, the NIR 4f–4f emissive complexes give typical 4f–4f emissions for the Nd(III), Tm(III) and Yb(III) complexes. Thus, it is seen that the energy transfer occurs from the SOMO π^* to the 4f excited level. These 4f–4f transitions are located below the NIT2py SOMO π^*. This behavior is similar to the case of the energy transfer from the $^2E(Cr^{III})$ to the 4f levels for the Cr–Nd and Cr–Yb dinuclear complexes [(acac)$_2$Cr(bpypz)Ln(hfac)$_3$] [65a,d], but different from that for the corresponding complexes [(acac)$_2$Cr(ox)Ln(HBpz$_3$)$_2$] which exhibit the simultaneous 3d–3d and 4f–4f luminescence at low temperature [65b,c,d]. As shown in Fig. 7 of Section 2.1.4, the NIT2py and IM2py radicals in the NIT2py and IM2py Cr(III) complexes exhibit the antenna effect, showing the fast energy transfer from the SOMO π^* to the $^2E/^2T_1(Cr^{III})$ state [42]. These findings suggest that the SOMO π^* doublet state of the nitroxide radical could be crucial for visible-light sensitization of NIR luminescence as a light harvesting antenna which could be required for possible candidates of NIR light sources. This is because of the lower lying of the NIT2py SOMO π^* band range existing within the emissive 4f levels than that of IM2py and NITBzImH or IMBzImH as shown in Fig. 14.

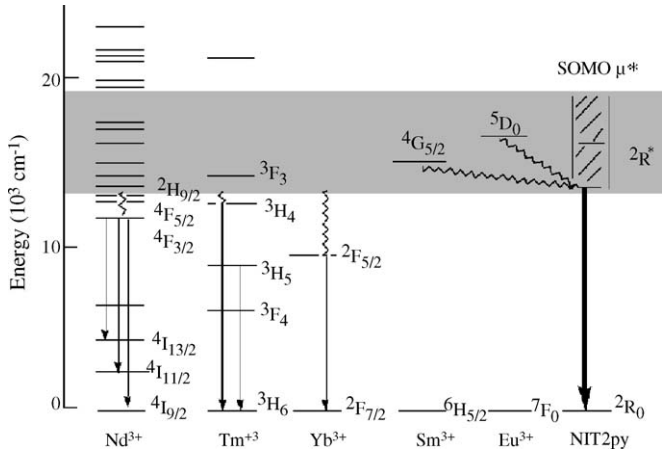

Fig. 14. Energy levels of NIR emissive and visible region emissive complexes and NIT2py (adapted from ref. [44]).

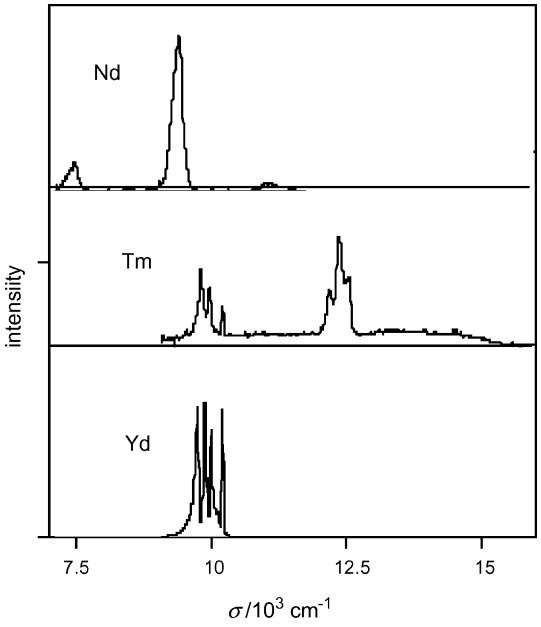

Fig. 15. Luminescence spectra in solid state at 15 K of [Ln(hfac)$_3$(NIT2py)] (top to bottom: Nd(III), Tm(III), Yb(III)) (adapted from ref. [44]).

Further photophysicochemical study will be awaited for development of new photosensitizers for NIR light sources which would make feasible by tuning the emissive states with variation of the substitution of NIT radical in nitroxide radical Ln(III) complexes.

5. Outlines and perspectives

The nitroxide radical ligands have been found to exhibit various coordination effects on the spectroscopic properties of the metal complexes, depending on the direct coordination of the nitroxide moiety or the indirect coordination through the pyridyl moiety or the magnetic d orbital symmetry or the kinds of the β-diketonate coligands.

The absorption band intensities in the spin-forbidden transitions for the Cr(III) and Ni(II) complexes with IM2py and NIT2py are enhanced in association with the new appearance of MLCT in the visible region. Such an intensity enhancement is elucidated in terms of the pair ion transition for the exchange mechanism; the formally spin-forbidden transitions and the MLCT between the same spin-multiplets. On the other hand, for the Cr(III) and Ni(II) β-diketonato complexes with IM2py and NIT2py, the larger difference of the J_{obsd} values with change of the β-diketonate coligands made it feasible to examine the origin of the magnetic interaction in relation with the variation of the absorption spectroscopic intensity and positions. For the Ni^{II}(IM2py), Cr^{III}(NIT2py) and Cr^{III}(IM2py) complexes, a large variation of the J_{obsd} is found to originate from the ferromagnetic interaction (J_F), but not from the antiferromagnetic interaction (J_{AF}). The reverse situation is encountered for the corresponding Ni(II) NIT2py complexes. Such a coligand effect arises from the electronic effect of the β-diketonates as revealed from the correlation with the Hammett constant (σ_m) of the substituents for the Ni^{II}(NIT2py) complexes or the Lewis acidity (pK_a) of the β-diketones themselves for the Ni^{II}(IM2py), Cr^{III}(NIT2py) and Cr^{III}(IM2py) complexes. The differences in magnitude of magnetic interactions among the Cr(III) and Ni(II) IM2py and NIT2py complexes are elucidated by considering the orthogonality or overlaps between the magnetic orbital (t_{2g} or e_g) and the SOMO π^*, LUMO π^* or HOMO π in the nitroxide radicals in terms of the VBCI description. Comparison of the magnetic interaction between the chelated and monodentate nitroxide radicals demonstrates that a necessary and sufficient condition for the intensity enhancement is not a large magnitude of J_{obs}, but rather the appearance of the MLCT bands due to the large overlap between the SOMO π^* and the d_π orbitals that augments the J_{ANT} values in terms of the exchange mechanism.

The magneto-optical properties of high-spin Co(II) complexes with each magnetic orbital in the t_{2g} and e_g subshells exhibit the coligand effects which bring about the different magnetic interaction and the MLCT band shifts arising from the change in electronic properties of the substituents with respect to their topological disposition.

Along with the d–d and CT transitions, the intraligand transitions are also influenced by the radical coordination as revealed by the absorption and luminescence spectra. It is likely that the observation of the mirror image between the absorption and luminescence spectroscopic patterns depends on the kinds of the nitroxide radicals. Unless there is no mirror image, two excited state of the SOMO is claimed with help of the DFT calculations by Reber, Luneau and co-workers. They also proposed the correlation between the luminescence patterns and the magnetic interaction with the nitroxide radicals. In this aspect, variable temperature MCD will be a promising tool to reveal the excited state of the nitroxide radical and the magnetic properties. For the monodentate radicals, there are found to be explicit perturbations on the $n \rightarrow \pi^*$ and $\pi \rightarrow \pi^*$ transition bands of the nitroxide moieties in the NIT*n*py and IM*n*py complexes of Co^{III} and Cr^{III} even with no significant structural and magnetic changes from the corresponding pyridine complexes and/or from free nitroxides. These perturbed properties may be related with the unusual diamagnetic ^{1}H NMR behavior of the radical ligands in the Co^{III}(IM3py or IM4py) and Ln^{III}(IM2py) complexes.

Observation of the singlet–triplet transition of the acetylacetonate in Ni(II)(IM2py) complexes and no observation in Ni(II) complexes excluding radical ligands may arise from the π^*(acetylacetonate)–π^*(IM2py) overlap for the LLCT and the orbital orthogonality between the magnetic e_g(Ni) and π^*(acetylacetonate) orbitals for the MLCT(Ni–acetylacetonate), respectively. At present, the simple approach in terms of the orbital symmetry consideration based on the orthogonality or overlap is valid to elucidate the electronic transitions between the same spin-multiplets in both the ground and excited states of the central metal as well as the ancillary ligand.

In view of no observation of the simultaneous 4f–4f and intraligand luminescence for the NIR emissive Ln(III) complexes in contrast to the case of the Eu complexes, the NIT2py in the NIR emissive Ln(III) complexes exhibits the antenna effect as a light harvesting ligand, which could be potential for visible-light sensitization required for possible candidates of NIR light sources. It is invaluable to clarify the difference between the doublet (SOMO π^*)-to-4f direct energy transfer in nitroxide Ln(III) complexes and the triplet-to-4f indirect one through intersystem crossing from singlet to triplet in non-radical organic ligands.

From a viewpoint of coordination chemistry including the relevant photochemistry and photophysics or material as well as biological sciences, more spectroscopic studies for various types of the nitroxide radical complexes must be awaited to understand electronic and magnetic properties or bonding in metal complexes with radical ligands by exploring the coordination effects of the radical ligands on the central metal ion with the d and/or f electrons.

In the future, it will become more invaluable to accumulate fundamental chiroptical information in order to clarify magneto-chiral effect leading to chiral magnets, for which the radical complexes have already been employed as promising targets.

Acknowledgements

I would like to express my sincere appreciation to all the collaborators whose names are given in the references as the co-authors. I also gratefully acknowledge support of our researches by a Grant-in-Aid for Scientific Research (No. 10304056) from

the Ministry of Education, Culture, Sports, Science, and Technology.

References

[1] H.U. Güdel, in: R.D. Willett, D. Gatteschi, O. Kahn (Eds.), Magneto-Structural Correlations in Exchange Coupled Systems., Reidel, Dordrecht, The Netherlands, 1985, p. 297.

[2] (a) P.J. McCarthy, H.U. Güdel, Coord. Chem. Rev. 88 (1988) 69 (and references therein);
(b) V.V. Eremenko, Magneto-Optics and Spectroscopy of Antiferromagnets, Springer, 1999;
(c) S. Sugano, N. Kojima, Magneto-Optics, Springer, 2000.

[3] O. Kahn, Struct. Bond. 68 (1987) 91 (and references therein).

[4] O. Kahn, Molecular Magnetism, VCH Publisher Inc., 1993.

[5] (a) J.S. Miller, A.J. Epstein, Angew. Chem. Int. Engl. 33 (1994) 385;
(b) J.S. Miller, Inorg. Chem. 39 (2000) 4392 (and references therein);
(c) A. Caneschi, D. Gatteschi, R. Sessoli, P. Rey, Acc. Chem. Res. 22 (1989) 392.

[6] (a) A. Caneschi, D. Gatteschi, P. Rey, Prog. Inorg. Chem. 39 (1991) 331 (and references therein);
(b) H. Iwamura, K. Inoue, T. Hayamizu, Pure Appl. Chem. 68 (1996) 243.

[7] E. Coronado, P. Delhaès, D. Gatteschi, J.S. Miller (Eds.), Molecular Magnetism: From Molecular Assemblies to the Devices, NATO ASI Series 321, Kluwer Academic Publishers, Dordrecht, 1996.

[8] (a) D.A. Shultz, Comments Inorg. Chem. 23 (2002) 1;
(b) D.A. Shultz, K.E. Vostrikova, S.H. Bodnar, H.-J. Koo, M.-H. Whangbo, M.L. Kirk, E.C. Depperman, J.W. Kampf, J. Am. Chem. Soc. 125 (2003) 1607;
(c) D.A. Shultz, Polyhedron 22 (2003) 2423.

[9] (a) E.I. Solomon, Inorg. Chem. 40 (2001) 3656;
(b) F. Tuczek, E.I. Solomon, Coord. Chem. Rev. 219–221 (2001) 1075 (and references therein).

[10] (a) A. Sokolowski, E. Bothe, E. Bill, T. Weyhermüller, K. Wieghardt, Chem. Commun. (1996) 1671;
(b) B. Adam, E. Bill, E. Bothe, B. Goerdt, G. Haselborst, K. Hildebrand, A. Sokolowski, S. Steenken, T. Weyhermüller, K. Wieghardt, Chem. Eur. J. (1997) 3;
(c) J. Muller, A. Kikuchi, E. Bill, T. Weyhermuller, P. Hildebrand, L. Ould-Moussa, K. Wieghardt, Inorg. Chim. Acta 297 (2000) 265 (and references therein).

[11] (a) C. Bellitto, P. Day, T.E. Wood, J. Chem. Soc., Dalton Trans. (1986) 847;
(b) C. Bellitto, P. Day, J. Chem. Soc., Dalton Trans. (1978) 1207;
(c) C. Bellitto, P. Day, J. Mater. Chem. 2 (1992) 265.

[12] (a) C. Mathonière, O. Kahn, J.C. Daran, H. Hilbig, F.H. Köhler, Inorg. Chem. 32 (1993) 4057;
(b) C. Mathonière, O. Kahn, Inorg. Chem. 33 (1994) 2103;
(c) O. Cador, C. Mathonière, O. Kahn, Inorg. Chem. 36 (1997) 1923;
(d) O. Cador, C. Mathonière, O. Kahn, Inorg. Chem. 39 (2000) 3799.

[13] P. Gütlich, Y. Garcia, H.A. Goodwin, Chem. Soc. Rev. 29 (2000) 419.

[14] (a) L. Dubicki, Aust. J. Chem. 25 (1971) 739l;
(b) J. Ferguson, H.U. Güdel, Aust. J. Chem. 26 (1972) 505;
(c) J. Ferguson, H.U. Güdel, M. Puza, Aust. J. Chem. 26 (1972) 513;
(d) A. Beutler, H.U. Güdel, T.R. Snellgrove, G. Chapuis, K.J. Schenk, J. Chem. Soc., Dalton Trans. (1979) 983;
(e) T. Tsubomura, I. Ohkouchi, M. Morita, Bull. Chem. Soc. Jpn. 64 (1991) 2341;
(f) T. Schönherr, J. Mol. Struct. (Theochem) 261 (1992) 203.

[15] (a) R. Schenker, H. Weihe, H.U. Güdel, Inorg. Chem. 38 (1999) 5593;
(b) R. Schenker, H. Weihe, H.U. Güdel, B. Kersting, Inorg. Chem. 40 (2001) 3355;
(c) R. Schenker, S. Heer, H.U. Güdel, H. Weihe, Inorg. Chem. 40 (2001) 1482.

[16] C. Benelli, A. Dei, D. Gatteschi, H.U. Güdel, L. Pardi, Inorg. Chem. 28 (1989) 3089.

[17] D. Luneau, G. Risoan, P. Rey, A. Grand, A. Caneschi, D. Gatteschi, J. Laugier, Inorg. Chem. 32 (1993) 5616.

[18] D. Luneau, P. Rey, J. Laugier, E. Belorizky, A. Cogne, Inorg. Chem. 31 (1992) 3578.

[19] (a) D. Luneau, J. Laugier, P. Rey, G. Ulrich, R. Ziessel, P. Legoll, M. Drillon, J. Chem. Soc., Chem. Commun. (1994) 741;
(b) D. Luneau, G. Risoan, P. Rey, A. Grand, A. Caneschi, D. Gatteschi, J. Langier, Inorg. Chem. 32 (1993) 5616.

[20] (a) F.M. Romero, D. Luneau, R. Ziessel, J. Chem. Soc., Chem. Commun. (1998) 551;
(b) D. Luneau, F.M. Romero, R. Ziessel, Inorg. Chem. 37 (1998) 5078.

[21] (a) D. Luneau, J. Laugier, P. Rey, G. Ulrich, R. Ziessel, P. Legoll, M. Drillon, J. Chem. Soc., Chem. Commun. (1994) 741;
(b) A. Marvilliers, Y. Pei, J.C. Boquera, K.E. Vostrikova, C. Paulsen, E. Rivière, J.-P. Audière, T. Mallah, Chem. Commun. (1999) 1951;
(c) K.E. Vostrikova, D. Luneau, W. Wernsdorfer, P. Rey, M. Verdaguer, J. Am. Chem. Soc. 122 (2000) 718.

[22] (a) M. Minguet, D. Luneau, E. Lhotel, V. Villar, C. Paulsen, D.B. Amabilino, J. Veciana, Angew. Chem. Int. Ed. 41 (2002) 586;
(b) K. Inoue, K. Kikuchi, N. Ohba, H. Okawa, Angew. Chem. Int. Ed. 42 (2003) 4210.

[23] (a) C. Hirel, J. Pécaut, S. Choua, P. Turek, D.B. Amabilino, J. Veciana, P. Rey, Eur. J. Org. Chem. 348 (2005) 359;
(b) M. Minguet, D.B. Amabilino, K. Wurst, J. Veciana, J. Chem. Soc., Perkin Trans. 2 (2001) 670;
(c) M. Minguet, D. Luneau, E. Lhotel, V. Vilar, C. Paulsen, D.B. Amabilino, J. Veciana, Angew. Chem. Int. Ed. 41 (2002) 586;
(d) M. Minguet, D.B. Amabilino, J. Vidal-Gancedo, K. Wurst, J. Veciana, J. Mater. Chem. 12 (2002) 570;
(e) M. Minguet, D. Luneau, C. Paulsen, E. Lhotel, A. Gorski, J. Waluk, D.B. Amabilino, J. Veciana, Polyhedron 22 (2003) 2349;
(f) M. Minguet, D.B. Amabilino, J. Veciana, Polyhedron 20 (2001) 1633;
(g) M. Minguet, D.B. Amabilino, K. Wurst, J. Veciana, J. Solid State Chem. 159 (2001) 440.

[24] (a) L. Dubicki, R.L. Martin, Aust. J. Chem. 22 (1969) 701;
(b) L. Dubicki, P. Day, Inorg. Chem. 11 (1972) 1868.

[25] J. Ferguson, H.J. Guggenheim, Y. Tanabe, J. Phys. Soc. Jpn. 21 (1966) 692.

[26] Y. Yamamoto, Y. Shimura, Bull. Chem. Soc. Jpn. 54 (1981) 3351.

[27] (a) T. Ohno, S. Kato, S. Kaizaki, I. Hanazaki, Chem. Phys. Lett. 102 (1983) 471;
(b) T. Ohno, S. Kato, S. Kaizaki, I. Hanazaki, Inorg. Chem. 25 (1986) 3853.

[28] P.W. Anderson, Phys. Rev. 115 (1959) 2.

[29] (a) H. Weihe, H.U. Güdel, Chem. Phys. Lett. 261 (1996) 123;
(b) H. Weihe, H.U. Güdel, Inorg. Chem. 36 (1997) 3632;
(c) H. Weihe, H.U. Güdel, H. Toftlund, Inorg. Chem. 39 (2000) 1351.

[30] F. Tuczek, E.I. Solomon, Inorg. Chem. 32 (1993) 2850.

[31] T. Yoshida, K. Kanamori, S. Takamizawa, W. Mori, S. Kaizaki, Chem. Lett. (1997) 603.

[32] (a) T. Yoshida, T. Suzuki, K. Kanamori, S. Kaizaki, Inorg. Chem. 38 (1999) 1059;
T. Yoshida, T. Suzuki, K. Kanamori, S. Kaizaki, Inorg. Chem. 38 (1999) 5926;
(b) T. Yoshida, S. Kaizaki, Inorg. Chem. 38 (1999) 1054.

[33] Y. Yamamoto, T. Suzuki, S. Kaizaki, J. Chem. Soc., Dalton Trans. (2001) 1566.

[34] Y. Yamamoto, T. Suzuki, S. Kaizaki, J. Chem. Soc., Dalton Trans. (2001) 2943.

[35] Y. Tsukahara, A. Iino, T. Yoshida, T. Suzuki, S. Kaizaki, J. Chem. Soc., Dalton Trans. (2002) 181.

[36] (a) M. Ogita, Y. Yamamoto, T. Suzuki, S. Kaizaki, Eur. J. Inorg. Chem. (2002) 886;
(b) T. Suzuki, M. Ogita, S. Kaizaki, Acta Crystallogr., Sect. C 56 (2000) 532.

[37] (a) T. Tsukuda, T. Suzuki, S. Kaizaki, J. Chem. Soc., Dalton Trans. (2002) 1721;

(b) T. Tsukuda, T. Suzuki, S. Kaizaki, Mol. Cryst. Liq. Cryst. 379 (2002) 159;
(c) T. Tsukuda, T. Suzuki, S. Kaizaki, Inorg. Chim. Acta 358 (2004) 1253;
(d) T. Tsukuda, M. Ogita, T. Suzuki, S. Kaizaki, Eur. J. Inorg. Chem. (2004) 4463.
[38] T. Tsukahara, T. Kamatani, A. Iino, T. Suzuki, S. Kaizaki, Inorg. Chem. 43 (2002) 4363.
[39] A. Iino, T. Suzuki, S. Kaizaki, Dalton (2003) 4604.
[40] Y. Tsukahara, T. Kamatani, T. Suzuki, S. Kaizaki, Dalton Trans. (2003) 1276.
[41] S. Kaizaki, Bull. Chem. Soc. Jpn. 76 (2003) 673.
[42] Y. Tsukahara, M. Nakata, S. Kaizaki, Inorg. Chem. 43 (2004) 4383.
[43] H. Kanda, Y. Narumi, Y. Hosokoshi, T. Suzuki, S. Kawata, K. Kindo, K. Inoue, S. Kaizaki, Inorg. Chim. Acta 357 (2004) 3125.
[44] S. Kaizaki, D. Shirotani, Y. Tsukahara, M. Nakata, Eur. J. Inorg. (2005) 3503.
[45] M. Kitano, Y. Ishimaru, K. Inoue, N. Koga, H. Iwamura, Inorg. Chem. 33 (1994) 6012.
[46] T. Schönherr, J. Mol. Struct. 261 (1982) 203.
[47] H.L. Schläfer, H. Gausmann, H.-U. Zander, Inorg. Chem. 6 (1967) 1528.
[48] A. Ceulemans, L.F. Chibotaru, G.A. Heylen, K. Pierloot, L.G. Vanquickenborne, Chem. Rev. 100 (2000) 787.
[49] F. Tuczek, E.I. Solomon, Coord. Chem. Rev. 219–221 (2001) 1075.
[50] D.F. Evans, J. Chem. Soc. (1957) 3885.
[51] M. Okutani, T. Yamuchi, T. Suzuki, S. Kaizaki, unpublished result.
[52] T. Ishida, T. Suzuki, S. Kaizaki, Inorg. Chim. Acta 357 (2004) 3134.
[53] T. Ishida, K. Adachi, S. Kawata, T. Suzuki, A. Fuyuhiro, S. Kaizaki, unpublished result.
[54] A. Bencini, C. Benelli, D. Gatteschi, Coord. Chem. Rev. 60 (1984) 131.
[55] R.L. Lintvedt, L.K. Kernitsky, Inorg. Chem. 9 (1970) 401.
[56] (a) C.K. Jørgensen, Modern Aspects of Ligand Field Theory, North-Holland Publ. Co., 1970;
(b) A.B.P. Lever, Inorganic Electronic Spectroscopy, Elsevier, 1984, pp. 209, 224.
[57] T. Yamauchi, S. Kaizaki, unpublished result.
[58] (a) A. Acosta, J.I. Zink, J. Cheon, Inorg. Chem. 39 (1999) 427;
(b) E. Wolcan, G. Torchia, J. Tocho, O.E. Piro, P. Juliarena, G. Ruiza, M.R. Féliz, J. Chem. Soc., Dalton Trans. (2002) 2194.
[59] (a) C. Lescop, D. Luneau, G. Bussière, M. Triest, C. Reber, Inorg. Chem. 39 (2000) 3740;
(b) C. Lescop, D. Luneau, P. Rey, G. Bussière, C. Reber, Inorg. Chem. 41 (2002) 5566.
[60] (a) C. Hirel, D. Luneau, J. Pécaut, L. Öhrström, G. Bussière, C. Reber, Chem. Eur. J. 8 (2002) 3157;
(b) R. Beaulac, G. Bussière, C. Reber, C. Lescop, D. Luneau, New J. Chem. 27 (2003) 1200;
(c) G. Bussière, R. Beaulac, H. Belisle, C. Lescop, D. Luneau, P. Rey, C. Reber, Top. Curr. Chem. 241 (2004) 97;
(d) C. Lescop, G. Bussière, R. Beaulac, H. Bélisle, E. Beloeizky, P. Rey, C. Reber, D. Luneau, J. Chem. Phys. Solid 65 (2004) 773;
(e) R. Beaulac, D. Luneau, C. Reber, Chem. Phys. Lett. 405 (2005) 153;
(f) D. Luneau, P. Rey, Coord. Chem. Rev. 249 (2005) 2591.
[61] T. Isobe, S. Kida, S. Misumi, Bull. Chem. Soc. Jpn. 40 (1967) 1862.
[62] (a) N. Sabbatini, M. Guardigi, J.-M. Lehn, Coord. Chem. Rev. 123 (1993) 201;
(b) H. Maas, A. Currao, G. Calzaferri, Angew. Chem. Int. Ed. 41 (2002) 2485;
(c) Y. Hasegawa, T. Ohkubo, K. Sogabe, Y. Kawamura, Y. Wada, N. Nakashima, S. Yanagida, Angew. Chem. Int. Ed. 39 (2000) 357.
[63] (a) S.I. Klink, L. Grave, L.D.N. Reinhoudt, F.C.J.M. van Veggel, M.H.V. Werts, F.A.J. Geurts, J.W. Hofstraat, J. Phys. Chem. A 104 (2000) 5457;
(b) G.A. Hebbink, L. Grave, L.A. Woldering, D.N. Reinhoudt, F.C.J.M. van Veggel, J. Phys. Chem. A 107 (2003) 2483;
(c) N.M. Shavaleev, S.J.A. Pope, Z.R. Bell, S. Faulkner, M.D. Ward, Dalton Trans. (2003) 808.
[64] F. Gutierrez, C. Tedeschi, L. Maron, J.-P. Daudey, R. Poteau, J. Azema, P. Tisnés, C. Picard, Dalton Trans. (2004) 1334.
[65] (a) R. Kawahata, T. Tsukuda, T. Yagi, M.A. Subhan, H. Nakata, A. Fuyuhiro, S. Kaizaki, Chem. Lett. (2003) 1084;
(b) M.A. Subhan, T. Suzuki, S. Kaizaki, Mol. Cryst. Liq. Cryst. 379 (2002) 395;
(c) M.A. Subhan, T. Suzuki, J.H. Choi, H. Nakata, S. Kaizaki, J. Lumin. 101 (2003) 307;
(d) M.A. Subhan, R. Kawahata, H. Nakata, A. Fuyuhiro, T. Tsukuda, S. Kaizaki, Inorg. Chim. Acta 357 (2004) 3139.